Post-translational Modifications of Human Thrombin-Activatable Fibrinolysis Inhibitor (TAFI): Evidence for a Large Shift in the Isoelectric Point and Reduced Solubility upon Activation†

Zuzana Valnickova,‡ Trine Christensen,‡ Peter Skottrup,‡ Ida B. Thøgersen,‡ Peter Højrup,§ and Jan J. Enghild*,‡

Center for Insoluble Protein Structure (inSPIN) at the Department of Molecular Biology, Science Park, University of Aarhus, Gustav Wied's Vej 10C, 8000 Aarhus C, Denmark, and Department of Biochemistry and Molecular Biology, University of Southern Denmark, Odense, Denmark

Received September 27, 2005; Revised Manuscript Received December 6, 2005

ABSTRACT: Thrombin-activable fibrinolysis inhibitor (TAFI) is distinct from pancreatic procarboxypeptidase B in several ways. The enzymatic activity of TAFIa is unstable and decays with a half-life of a few minutes. During this study, we observed that (i) the isoelectric point (pI) of TAFI shifts dramatically from pH 5 toward pH 8 upon activation and (ii) TAFIa is significantly less soluble than TAFI. The structural bases for these observations were investigated by characterizing all post-translational modifications, including attached glycans and disulfide connectivity. The analyses revealed that all five potential N-glycosylation sites were utilized including Asn22, Asn51, Asn63, Asn86 (located in the activation peptide), and Asn219 (located in the catalytic domain). Asn219 was also found in an unglycosylated variant. Four of the glycans, Asn51, Asn63, Asn86, and Asn219 displayed microheterogeneity, while the glycan attached to Asn22 appeared to be homogeneous. In addition, bisecting GlcNAc attached to the trimannose core was detected, suggesting an origin other than the liver. Monosaccharide composition and LC−MS/MS analyses did not produce evidence for O glycosylation. TAFI contains eight cysteine residues, of which two, Cys69 and Cys383, are not involved in disulfides and contain free sulfhydryl groups. The remaining six cystines form disulfides, including Cys156−Cys169, Cys228−Cys252, and Cys243−Cys257. This pattern is homologous to pancreatic procarboxypeptidase B, and it is therefore unlikely that permutations in the cysteine connectivity are responsible for the enzymatic instability. LC−MS/MS analyses covering more than 90% of the TAFI amino acid sequence revealed no additional modifications. When these results are taken together, they suggest that the inherent instability of TAFIa is not caused by post-translational modifications. However, after activation, TAFIa loses 80% of the attached glycans, generating a large shift in pI and a propensity to precipitate. These changes are likely to significantly affect the properties of TAFIa as compared to TAFI.

Thrombin-activatable fibrinolysis inhibitor (TAFI)[1] (EC 3.4.17.20; UniProt, Q96IY4), also known as plasma procarboxypeptidase B, R, and U, was first identified as a plasma carboxypeptidase that interfered with carboxypeptidase N assays (*1*−*3*). Later, the protein was purified, and the cDNA sequence was determined (*4*). TAFI was purified by plasminogen affinity chromatography, and this property led investigators to explore a role in fibrinolysis (*5*−*11*). A splice variant of TAFI has been termed "brain carboxypeptidase B" and might play a role in the degradation of β-amyloid 1−42 (*12*), and it has been shown that a Thr325Ile mutation affects the outcome of meningococcal disease (*13*).

TAFI is a single chain, 60-kDa glycoprotein secreted by the liver. The protein belongs to the metallocarboxypeptidase family (EC 3.4.17), displaying a high degree of sequence identity with carboxypeptidases A and B (*14*−*17*). This identity includes residues responsible for substrate binding, Arg235, Tyr341, and Asn234, the catalytic region, Glu363 and Arg217, and the zinc-binding region, His159, Glu162, and His288 (all TAFI zymogen numbering) (*4*, *18*). It has been speculated that TAFI circulates in a complex with plasminogen (*9*). The affinity of TAFIa for plasminogen is reduced, and because the molecular mass is below the glomerular filtration limit, the active enzyme might be retained in the circulation by binding to α_2-macroglobulin or pregnancy zone protein (*19*). In addition TAFI and TAFIa are substrates for transglutaminases, suggesting that they are cross-linked to fibrin during coagulation (*20*). TAFIa down-regulates fibrinolysis by removing C-terminal lysine residues

† The work was supported by grants from the Danish Natural Science Research Council (to J.J.E.). P.S. and T.C. were recipients of scholarships from the Danish Cancer Society and Novo Nordisk Foundation.

* To whom correspondence should be addressed: Department of Molecular Biology, University of Aarhus, Gustav Wied's Vej 10C, 8000 Aarhus C, Denmark. Telephone: +45-8942-5062. Fax: +45 8942 5063. E-mail: jje@mb.au.dk.

‡ University of Aarhus.

§ University of Southern Denmark.

[1] Abbreviations: AMAC, 2-aminoacridone; FACE, fluorophore-assisted carbohydrate electrophoresis; Fuc, fucose; Gal, galactose; NeuAc, *N*-acetyl neuraminic acid; GalNAc, *N*-acetylgalactosamine; GlcNAc, *N*-acetylglucosamine; MALDI−TOF MS, matrix-assisted laser desorption ionisation−time-of-flight mass spectrometry; Man, mannose; PAGE, polyacrylamide gel electrophoresis; PVDF, poly(vinylidene difluoride); RP-HPLC, reverse-phase high-performance liquid chromatography; TAFI, thrombin-activatable fibrinolysis inhibitor; TFA, trifluoroacetic acid; SPase V8, *Staphylococcus aureus* V8 protease.

10.1021/bi051956v CCC: $33.50
Published on Web 01/12/2006

exposed on the surface of the fibrin clot (*9*, *21*). Elimination of these plasminogen and tissue-type plasminogen activator (t-PA) binding sites disrupts the t-PA-mediated plasminogen activation, resulting in a decreased rate of plasmin generation, downregulation of fibrinolysis, and stabilization of the fibrin clot (*22*−*26*).

Activation is achieved by proteolysis of the Arg92−Ala93 peptide bond. This removes the activation peptide and generates the active form (*4*, *27*). Several proteases activate TAFI *in vitro*, including trypsin (*4*), thrombin (*6*), and plasmin (*4*, *28*). The thrombin/thrombomodulin complex is a likely activator of TAFI *in vivo* (*6*), although plasmin may also be able to function as a physiological activator (*28*).

In contrast to the homologous pancreas carboxypeptidase B, the enzymatic activity of TAFIa is unstable, with a half-life ranging from 1.4 to 15 min at 37 °C depending upon the isoform (*29*, *30*). The molecular mechanism responsible for the instability is unclear but is not exclusively caused by proteolytic degradation, because TAFI mutants resistant to adventitious proteolysis remain unstable (*29*, *30*). Alternatively, it has been suggested that the rapid decay of enzymatic activity is caused by thermodynamic instability following activation (*31*). This is cooperated by the temperature-dependent decay of TAFIa activity, where the activity is essentially stable at 4 °C. Other clues have been provided by studying naturally occurring TAFI variants and mutants. The Ala147Thr variant displays the same enzymatic endurance as the wild type (*32*), but the Thr325Ile substitution increases the half-life from 8 to 15 min (*33*, *34*). Mutations of Arg302Gln, Arg320Gln, and Arg330Gln produced a molecule less stable then the wild type. These results indicate that a region including residues 302−330 may be important for the stability (*29*, *34*). Others have suggested that hydrophobic residues, Ile90−Ile91, likely located in an exposed loop unique to TAFI may contribute to destabilizing the structure of TAFIa (*35*).

In the absence of crystallographic data, structural explanations for the inherent instability of TAFIa were pursued by characterizing all post-translational modifications. The protein was analyzed by LC−MS/MS, and the post-translational modifications were limited to N-linked glycans and disulfides. The disulfides were homologous to procarboxypeptidase B, suggesting that an alteration in the disulfide-bridge connectivity is not the reason for the reduced enzymatic endurance of TAFIa. The glycans were mainly associated with the activation peptide, and TAFIa underwent a large shift in pI and a significant reduction in solubility. The shift in pI and the reduced solubility are likely to significantly impact the properties of TAFIa, particularly by modulating protein−protein interactions.

EXPERIMENTAL PROCEDURES

Proteins. TAFI was purified from normal human plasma (Statens Serum, Institute, Copenhagen, Denmark) using plasminogen-depleted plasma (*36*) and Plasminogen-Sepharose affinity chromatography (*4*, *19*). Recombinant soluble thrombomodulin (solulin) was a generous gift of Dr. Achim Schuettler (PAION GmbH, Aachen, Germany). TAFI antiserum was raised commercially (Pel-Freez, Rogers, AR).

Polyacrylamide Gel Electrophoresis (PAGE) and Western Blotting. Proteins were separated by SDS−PAGE in 5−15% polyacrylamide gels (*37*). Prior to electrophoresis, samples were boiled for 5 min in the presence of 30 mM dithiothreitol (DTT) and 1% SDS. For Western blotting, proteins were electrophoretically transferred to a poly(vinylidene difluoride) (PVDF) membrane as described before (*38*). The membranes were blocked with 5% (w/v) skimmed milk in 20 mM Tris-HCl and 150 mM NaCl at pH 7.4. TAFI was detected by enhanced chemiluminescence (Amersham Biosciences) using an rabbit anti-human TAFI antiserum and HRP-conjugated goat anti-rabbit Ig.

One-Dimensional Isoelectric Focusing (IEF). IEF was performed using Ready Gel Precast IEF polyacrylamide gel (BioRad) containing ampholine with a pH range of 3−10. The gels were placed in a Mini-Protein 3 Cell, as described by the manufacturer (BioRad). Gels were developed using IEF-staining solution composed of 27% isopropyl alcohol, 10% acetic acid, 0.04% Coomassie Blue R250, and 0.05% Crocein Scarlet in H_2O.

Activation of Human TAFI. Human TAFI was activated by trypsin or thrombomodulin (solulin)/thrombin. The trypsin activation was achieved as described previously (*19*). In short, TAFI was incubated for 20 min at 37 °C using a trypsin/TAFI (w/w) ratio of 0.5:1 in 20 mM Tris-HCl and 100 mM NaCl at pH 7.5. The activation was followed by the carboxypeptidase B activity assay described previously (*39*) and SDS−PAGE (*37*). The thrombomodulin (solulin)/thrombin activation of TAFI was carried out by incubating 2 μg of TAFI and a complex composed of 1 μg of solulin and 0.04 μg of thrombin for 30 min in 20 mM Tris-HCl and 100 mM NaCl at pH 7.5 and 25 °C.

Reduction and Alkylation. Samples were reduced in 20 mM NH_4HCO_3 at pH 8. DTT was added (final concentration of 15 mM), and the samples were incubated at 21 °C for 20 min. The reduced samples were alkylated for 20 min at 21 °C using 15 mM iodoacetamide. Some samples were alkylated without prior reduction.

Deglycosylation of TAFI. Aliquots of reduced and alkylated TAFI in 50 mM $NaHPO_4$ at pH 7.5 containing 50 mM DTT and 0.1% (w/v) SDS were boiled for 5 min. The samples were allowed to cool before adding 0.75% (v/v) Triton X-100 and PNGase F (final concentration from 0 to 100 mU). Deglycosylation was allowed to proceed for 3 h at 37 °C before the reaction products were analyzed by SDS−PAGE. Gels were stained with Coomassie Brilliant Blue. Deglycosylated peptides were desalted using μC-18 zip tips (Millipore Coorporation). To investigate the solubility of deglycosylated protein, TAFI was incubated with PNGase F (100 mU) under native conditions. Incubation proceeded overnight at 37 °C before the sample was centrifuged (13000*g*, 15 min), and both the pellet and supernatant were analyzed by SDS−PAGE.

Monosaccharide Composition. The monosaccharide composition was determined by fluorophore-assisted carbohydrate electrophoresis (FACE) using a monosaccharide composition kit (Prozyme, Glyco). Briefly, for approximately 3 times, 15 μg of TAFI was subjected to SDS−PAGE, transferred to a PVDF membrane (*38*), and stained with Coomassie Blue. The protein bands were excised and subjected to three separate hydrolysis reactions: (i) 0.1 N trifluoroacetic acid (TFA) at 80 °C for 1 h to release sialic acid, (ii) 2 N TFA at 100 °C for 5 h to release neutral sugars, and (iii) 4 N HCl at 100 °C for 3 h to release amine sugars.

The released monosaccharides were labeled overnight with the fluorophore, 2-aminoacridone (AMAC), and resolved on a proprietary gel system. After electrophoresis, the gels were imaged using a fluorescence camera linked to a computer. The data were analyzed using proprietary software.

Enzymatic Digestions. Aliquots of alkylated TAFI were digested using endoproteinase AspN (Roche), chymotrypsin (Promega), or porcine trypsin (Promega). Some peptides were subdigested using *Staphylococcus aureus* V8 protease (SPase V8; Roche Applied Science). The enzyme/substrate ratios were between 1:20 and 1:40. The digestions were carried out at 37 °C for 17 h in 50 mM NaH_2PO_3 at pH 8 or 20 mM NH_4HCO_3 at pH 8. For some experiments, TAFI was reduced and alkylated prior to digestion.

Peptide Purification. Peptides were purified by reverse-phase high-performance liquid chromatography (RP-HPLC) using various columns supplied by Applied Biosystems (Aquapore RP-300 column, 2.1 × 220 mm) and Phenomenex (Jupiter C18 column, 2.0 × 250 mm) A Pharmacia SMART system was used to form linear gradients from 0.1% TFA (buffer A) to 90% acetonitrile and 0.08% TFA (buffer B). The peptides were detected at 220 nm and collected manually.

Purification of Glycosylated Peptides. Reduced and alkylated TAFI digests were applied separately to a 2 mL concanavalin A column (Amersham Biosciences) connected to a Pharmacia SMART system (Amersham Biosciences), at a flow rate of 200 μL/min. The column was washed in 20 mM Tris-HCl, 0.5 M NaCl, 1 mM $CaCl_2$, and 1 mM $MnCl_2$ at pH 7.4 and eluted using the same buffer containing 0.5 M methyl-α-D-glucopyranoside) at 100 μL/min. The glycosylated peptides were collected, acidified, and further purified by RP-HPLC. The relative levels of the individual peptide glycovariants were estimated on the basis of the absorbance at 220 nm.

Isolation of Cysteine-Containing Peptides. Alkylated but nonreduced TAFI was digested, and the peptides were separated by gel-filtration chromatography using Superdex Peptide HR 10/30 column (Amersham Biosciences). The column was equilibrated in 20 mM Na_3PO_4 at pH 7.2 and 250 mM NaCl and connected to a Pharmacia SMART system (Amersham Biosciences). Fractions were pooled, acidified, and further separated by RP-HPLC. The peptides were analyzed by Edman degradation and MALDI−MS to verify disulfide or free cysteine residues.

N-Terminal Amino Acid Sequencing. Peptides destined for N-terminal sequence analyses were applied to a Biobrene precycled glass-fiber filter (Applied Biosystems) and subjected to automated Edman degradation in an Applied Biosystems Model 477A sequencer with on-line phenylthiohydantoin analysis using an Applied Biosystems Model 120A HPLC system.

Characterization of Glycosylated Peptides by Matrix-Assisted Laser Desorption Ionization−Mass Spectroscopy (MALDI−MS). Glycopeptides were analyzed by MALDI−MS using a Perseptive Voyager DE-PRO mass spectrometer MALDI−TOF instrument (Applied Biosystems). The spectra were recorded in linear or reflectron modes of operation by averaging 50 or 100 laser shots depending upon the nature of the sample. The mass accuracy in the reflectron mode with external calibration was typically better than 50 ppm. Time-to-mass conversion was achieved by external calibration using angiotensin II (1296.68 Da) and adrenocorticotropin(18−39)−peptide (2466.71 Da). All experiments were performed using α-cyano-4-hydroxycinnamic acid (Sigma) as the matrix. Saturated matrix solutions were prepared in 70% acetonitrile/0.1% TFA, mixed in equal volumes with peptide samples, and applied on the MALDI target plate. The expected mass of peptides and proteins was calculated using General Protein/Mass Analysis for Windows (GPMAW) software (Lighthouse data, Odense, Denmark). Selected glycopeptides were further treated with neuraminidase to determine *N*-acetylneuraminic acid content. The peptides were dried-down and redissolved in 0.1 M sodium acetate at pH 6.0. A total of 66 mU of neuraminidase was added, and samples were left to incubate for 16 h at 37 °C. Buffer salts were removed on μC18 ZipTips (Millipore), and the sample eluted directly onto the MALDI−TOF target plate with 4 mg/mL α-cyano-4-hydroxycinnamic acid in 50% acetonitrile/water.

MALDI−MS of Cys Peptides. Cysteine-containing peptides were analyzed by MALDI−MS using a Micromass Q-TOF Ultima Global mass spectrometer (Micromass, Manchester, U.K.), operated in reflectron MALDI−MS mode. All experiments were performed using α-cyano-4-hydroxycinnamic acid (Sigma) as the matrix. The expected mass of peptides and proteins was calculated using General Protein/Mass Analysis for Windows (GPMAW) software (Lighthouse data, Odense, Denmark). All numbering and calculations are based on the TAFI sequence as reported in UniProt (Q96IY4) without the initial 22-residue signal sequence.

Electrospray Ionization (ESI) Mass Spectrometry. The LC−MS/MS analyses were performed using a Micromass Q-TOF Ultima Global mass spectrometer connected to an LC-Packings UltiMate Nano LC system with autosampler. A nanospray ion source was used to hold the packed fused-silica emitters and to apply capillary voltage through a Valco union. Injected samples were first trapped and desalted isocratically on a LC-Packings PepMap C18 Precolumn cartridge (300 μm × 1 mm). The peptides were eluted and separated on an analytical fused-silica emitter (New Objective, 10 cm × 75 μm, packed with Zorbax, 300SB, C18, Agilent Technologies) connected in-line to the mass spectrometer. The column was developed using a 200 nL/min flow rate and linear gradients from buffer A (0.02% HFBA and 0.5% acetic acid in water) to buffer B (0.02% HFBA, 0.5% acetic acid, and 75% acetonitrile in water). After data acquisition, the individual MS/MS spectra acquired for each precursor were combined, smoothed, deisotoped, and compiled as a single Mascot-searchable peak list. The peak-list files were used to query the Swiss-Prot database using the Mascot program. Unmatched spectra were analyzed using the Mascot error-tolerant search option (*40*).

RESULTS

TAFI Undergoes a Large Shift in the Isoelectric Point (pI) upon Activation. TAFI and TAFIa were analyzed by IEF (Figure 1). The zymogen migrated as several bands between pI 4.8 and 5.5. TAFIa was more homogeneous, and only one band was apparent. Significantly, the pI of TAFIa was around 8. Because the theoretical pI of TAFI is around 8.5 and that of TAFIa is around 8.9, this indicates a strong influence of sialic acid. The loss of the heavily glycosylated

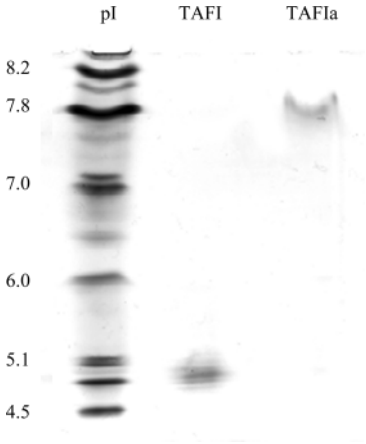

FIGURE 1: Isoelectric focusing of TAFI and TAFIa. TAFI was activated using thrombin−thrombomodulin (solulin), and approximately 10 μg of TAFI and TAFIa was focused under native conditions, using a pH 3−10 gradient as indicated. The protein bands were visualized by staining with Coomassie Blue and Crocein Scarlet. It is apparent that TAFI undergoes a large shift in the pI from approximately 5 to 8 following activation.

activation peptide is the most likely explanation for this shift in pI. The migration pattern is consistent with that of a heterogeneously glycosylated protein. This large shift in pI from an acidic to a basic protein is likely to change the binding properties and protein interaction profile of TAFIa.

Effect of the Carbohydrate on Solubility. To investigate if the carbohydrate moieties affected the solubility, TAFI was enzymatically deglycosylated. The products were centrifuged, and the pellet and supernatant were analyzed separately by reduced SDS−PAGE (Figure 2A). The result showed that the majority of TAFI was in the pellet, suggesting that the carbohydrate was important for the solubility of TAFI. The activation of TAFI releases the activation peptide containing the majority of the attached glycans, indicating that TAFIa similarly will exhibit reduced solubility. To test this, TAFI was activated using thrombin−thrombomodulin (solulin) centrifuged as described above and analyzed by reduced SDS−PAGE (Figure 2B). Examination of the gel revealed that a significant portion of TAFIa was in the pellet, suggesting reduced solubility following activation.

TAFI Contains N-Linked Glycosylation Only. To further analyze the structural properties of the attached glycans, the monosaccharide composition was determined (Figure 3A). Identification of *N*-acetylgalactosamine (GalNAc) is indicative of the presence of O-linked carbohydrates; however, no GalNAc was observed. The presence of mannose (Man), fucose (Fuc), galactose (Gal), *N*-acetyl neuraminic acid (NeuAc), and *N*-acetylglucosamine (GlcNAc) suggested the presence of N-linked glycans. In compliance with this, TAFI contains five potential N-glycosylation sites (Asn-XXX-Ser/Thr/Cys), including Asn22, Asn51, Asn63, Asn86, and Asn219.

All Five Glycosylation Sites in TAFI Are Utilized. TAFI was deglycosylated with PNGase F using limited conditions. The reaction products were analyzed by reduced SDS−PAGE and generated a "ladder" of partially digested TAFI, containing a total of five bands, with the lowest band approaching the theoretical mass (46 kDa) of TAFI zymogen

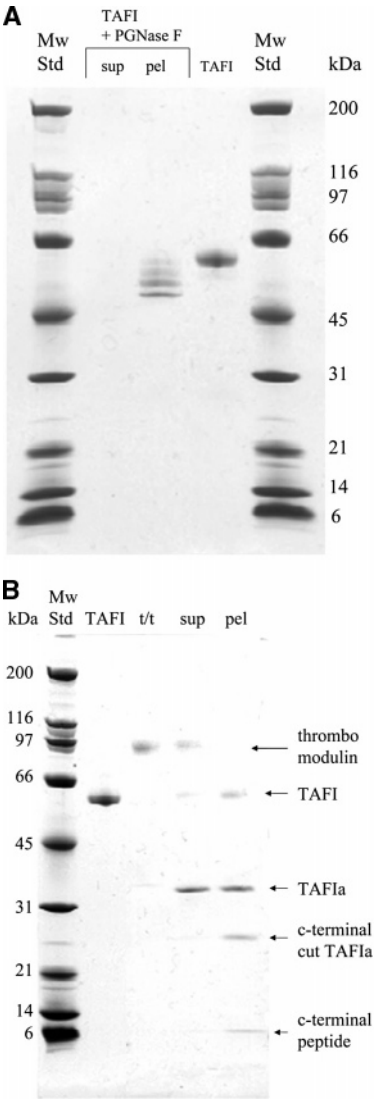

FIGURE 2: (A) Deglycosylated TAFI is insoluble. TAFI was enzymatically deglycosylated using PNGase F under native conditions. After deglycosylation, the protein was centrifuged and the supernatant (sup) and pellet (pel) were analyzed by reduced SDS−PAGE. TAFI zymogen is shown as a control (TAFI). Because the reaction was performed using native conditions, the deglycosylation did not go to completion. However, the experiments show that deglycosylated and partially deglycosylated TAFI products were insoluble. (B) TAFIa is significantly less soluble than TAFI. Because four of the five N-linked glycan attachment sites are located on the activation peptide, we investigated the solubility of the TAFIa. TAFI was activated using thrombin−thrombomodulin (solulin) and centrifuged. The supernatant (sup) and pellet (pel) were analyzed by reduced SDS−PAGE. The different reaction products of the TAFI activation are indicated. TAFI zymogen (TAFI) and thrombin−thrombomodulin (t/t) alone are shown for a comparison. The experiment revealed that a large portion of TAFIa is in the pellet, suggesting that the activated enzyme is significantly less soluble that TAFI.

(Figure 3B). This indicates that all potential N-linked glycosylation sites are utilized.

Isolation and Identification of N-Glycosylated Peptides. To establish the structure of the attached glycans, peptides containing only one potential N-glycosylation site were produced using protease AspN alone or in combination with trypsin. The N-glycosylated peptides were affinity-purified on a concanavalin A column (data not shown), followed by RP-HPLC (parts A and B of Figure 4). The purified peptides

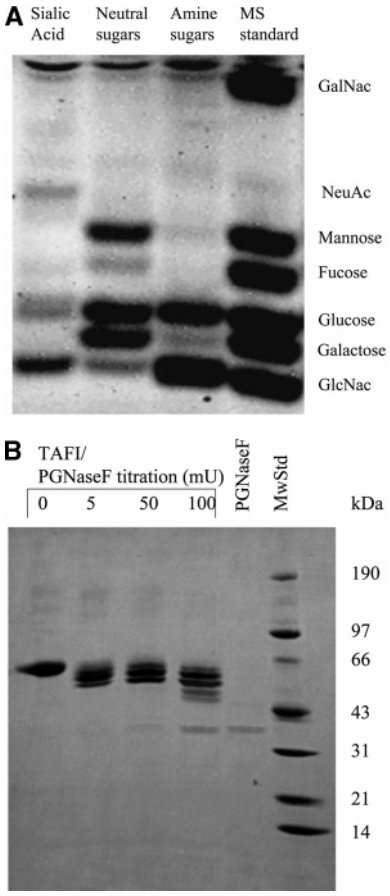

FIGURE 3: (A) Monosaccharide composition of TAFI. The monosaccharide composition of TAFI glycans was determined by FACE monosaccharide composition kit (Glyco). Three different hydrolysis conditions were used, specific for either NeuAc, neutral sugars, or amine sugars, as described in the Experimental Procedures. The monosaccharide standard (MS standard) was composed of a mixture of fluorophore-labeled monosaccharides, GalNAc, Man, Fuc, glucose, Gal, and GlcNAc. All monosaccharides were found in the TAFI carbohydrate, except GalNAc, suggesting that TAFI is not O-glycosylated. (B) All five potential TAFI N-linked glycosylation sites are used. TAFI was incubated with increasing amounts of PNGase F as indicated and analyzed by reduced SDS−PAGE. Each band contains at least one N-linked chain less than the band above. Close examination of the band pattern revealed a "5 stepladder", suggesting the presence of five N-linked chains.

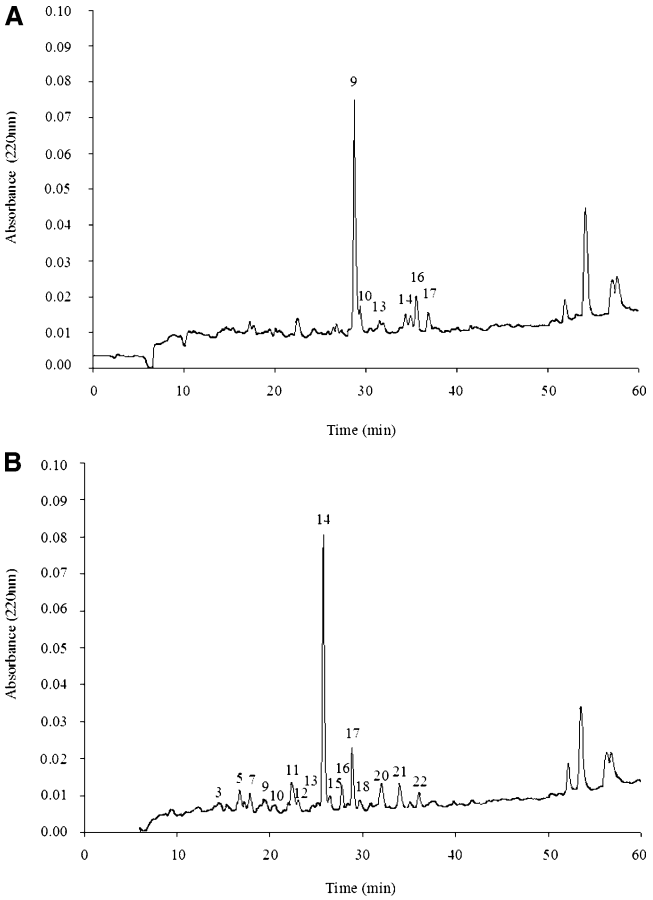

FIGURE 4: (A) Purification of glycosylated TAFI peptides following digestion with AspN. The AspN digest was applied to a Concavalin A column. The adsorbed peptides were eluted, purified by RP-HPLC, and analyzed by MALDI−MS and Edman degradation. (B) Isolation of glycosylated peptides following digestion with both AspN and trypsin. The numbers shown above each peak correlate with the fraction numbers listed in Table 1.

were subsequently analyzed by MALDI−TOF and Edman degradation when required (Table 1). Sialylated glycans often show a characteristic fragmentation pattern in MALDI−TOF, typified by the loss of 292 Da. To simplify the mass spectra and characterize the complexity of attached NeuNAc, each glycopeptide was analyzed by MALDI−TOF MS before and after digestion with neuraminidase (Table 1). All five potential N-glycosylation sites were confirmed, utilized by MALDI−TOF MS. The Asn219 site was furthermore found in a nonglycosylated form (data not shown) producing an unglycosylated TAFIa variant.

Structure of the Asn22-Linked Glycan. The Asn22 glycan appeared to be homogeneous. The expected mass of the AspN peptide was 2543.36 Da, and the observed masses of 6265.80, 5973.08, 5687.67, 5388.94, and 5100.26 Da (Table 1) are consistent with a tetra-antennary complex type, bisecting the GlcNAc structure (0−4 NeuNAc) (Figure 6). The NeuNAc heterogeneity was removed by neuraminidase treatment (5096.60 Da), further confirming the proposed structure (Table 1 and Figure 6).

Structures of Asn51-Linked Glycans. The glycans attached to Asn51 were heterogeneous, and both hybrid- and complex-type glycans were detected (Table 1 and Figure 6). Hybrid-type glycans were identified including mono-antennary structures containing 3−8 Man (5%), di-antennary structures with 6−7 Man (62%), di-antennary with a bisecting GlcNAc, six Man, and one Fuc (5%), di-antennary with a bisecting GlcNAc, seven Man, and two Fuc (10%). In addition, complex-type glycosylation was identified; di-antennary (6%), bi-antennary with a bisecting GlcNAc and Fuc (2%), tri-antennary with Fuc (5%), and a penta-antennary structure with Fuc (5%) (Figure 6). In general, the proposed structures were verified by neuraminidase treatment (Table 1).

Structures of Asn63-Linked Glycans. Three different types of structures attached to Asn63 were determined (Table 1 and Figure 6), a hybrid-type mono-antennary with bisecting GlcNAc and 4−6 Man attached (23%) and a hybrid-type mono-antennary with six Man and two Fuc (54%). The third type of structure was a tri-antennary complex-type structure with a bisecting GlcNAc and two Fuc (23%). Again, all proposed structures were verified by neuraminidase treatment (Table 1).

Structures of Asn86-Linked Glycans. The glycans attached to Asn86 likewise displayed microheterogeneity (Figure 6).

Table 1: Identification of N-Linked Carbohydrate Structures

glyco site	peptide and enzyme used	HPLC fraction	molecular mass of peptide (Da)			molecular mass after neuraminidase (Da)		proposed carbohydrate attached
			theoretical without carbohydrate	observed	theoretical with carbohydrate	observed	theoretical	
Asn^{22}	$Gln^{16}-Ala^{37}$ AspN/Tryp	7	2543.36	6265.80 5973.08 5687.67 5388.94 5100.26	6267.32 5976.07 5684.81 5393.55 5102.29	5096.60	5102.29	complex tetra-antennary bisecting GlcNAc + 0−4 NeuAc
Asn^{51}	$Gln^{45}-Ser^{53}$ AspN/Tryp	5	1048.17	3249.71 2957.47 2795.68 2633.26	3246.15 2954.89 2792.75 2630.61	2959.68 2797.88 2635.23	2954.89 2792.75 2630.70	hybrid mono-antennary 5−7 mannose + 0−1 NeuAc
Asn^{51}	$Gln^{45}-Ser^{53}$ AspN/Tryp	10	1048.17	3410.03 3247.06 2928.05 2765.88 2603.48	3408.29 3246.15 2921.86 2759.72 2597.58	ND	3117.04 2954.89 2630.61 2468.47 2306.32	hybrid mono-antennary 3−8 mannose 1 NeuAc
Asn^{51}	$Gln^{45}-Ser^{53}$ AspN/Tryp	12	1048.17	3085.04 2927.03 2763.87	3084.01 2921.86 2759.72	ND	2792.75 2630.61 2468.47	hybrid mono-antennary 4−6 mannose 1 NeuAc
Asn^{51}	$Gln^{45}-Ser^{53}$ AspN/Tryp	15	1048.17	3607.50 3319.48 3027.41	3603.51 3312.25 3021.00	3027.00 3336.44 (incomplete digest + oxidation)	3021.00	complex di-antennary bisecting GlcNAc 1 fucose + 0−2 NeuAc
Asn^{51}	$Gln^{45}-Ser^{53}$ AspN/Tryp	16	1048.17	3256.50 2964.45 2679.40	3254.17 2962.92 2671.66	2675.21 2967.71 (incomplete digest)	2671.66	complex di-antennary + 0−2 NeuAc
Asn^{51}	$Gln^{45}-Ser^{53}$ AspN/Tryp	18	1048.17	3258.10 2967.00 2675.00	3254.17 2962.92 2671.66	2676.40	2671.66	complex di-antennary + 0−2 NeuAc
Asn^{51}	$Gln^{45}-Ser^{53}$ AspN/Tryp	20	1048.17	$4513.09 + Na^+$ $4223.44 + Na^+$ $3933.30 + Na^+$	4496.33 4205.07 3913.81	$3932.75 + Na^+$	3913.81	complex penta-antennary 1 fucose + 0−2 NeuAc
Asn^{51}	$Gln^{45}-Ser^{53}$ AspN/Tryp	21	1048.17	3759.87 3468.40 3176.00	3765.65 3474.40 3183.14	3176.98	3183.14	complex tri-antennary 1 fucose + 0−2 NeuAc
Asn^{51}	$Asp^{38}-Ser^{53}$ AspN	9	1873.23	4565.2 4271.1 3979.6	4565.66 4274.71 3983.15	3980.30	3983.15	hybrid di-antennary 6 mannose + 0−2 NeuAc
Asn^{51}	$Asp^{38}-Ser^{53}$ AspN	10	1873.23	4724.1 4563.1 4271.5	4727.81 4565.66 4274.41	3979.41 4565.66 4274.41	3983.15 4145.29	hybrid di-antennary 6−7 mannose + 0−2 NeuAc
Asn^{51}	$Asn^{38}-Ser^{53}$ AspN	13	1873.23	4910.96 4619.98 4327.90	4915.00 4623.74 4332.49	ND	4332.49	hybrid di-antennary bisecting GlcNAc 6 mannose 1 fucose + 0−2 NeuAc
Asn^{51}	$Asp^{38}-Ser^{53}$ AspN	16	1873.23	5224.30 4933.10 4639.60	5223.29 4932.03 4640.77	4642.34	4640.77	hybrid di-antennary bisecting GlcNAc 7 mannose 2 fucose + 0−2 NeuAc
Asn^{63}	$Ala^{60}-Ala^{74}$ AspN/Tryp	7	1492.78	3731.04 3439.82 3277.85 3115.62	3731.82 3440.56 3278.42 3116.28	3440.40 3278.50 3116.40	3440.56 3278.42 3116.28	hybrid mono-antennary bisecting GlcNAc 4−6 mannose + 0−1 NeuAc
Asn^{63}	$Asp^{56}-Ala^{74}$ AspN	17	1949.04	4850.10 4563.20 4279.92	4861.92 4570.66 4279.40	4270.15	4279.40	hybrid mono-antennary 6 mannose 2 fucose + 0−2 NeuAc
Asn^{63}	$Ala^{60}-Ala^{74}$ AspN/Tryp	22	1492.78	4325.00 4034.37 3742.52	4325.38 4034.12 3742.87	3741.2 (incomplete digest)	3451.61	complex tri-antennary bisecting GlcNac only one galactose 2 fucose + 1−3 NeuAc
Asn^{86}	$Asp^{78}-Asn^{86}$ AspN/Tryp	13	1058.16	3920.60 3628.40 3336.40	3920.76 3629.50 3338.24	3335.70 (incomplete digest)	3046.99	complex tri-antennary + 1−3 NeuAc

Table 1: (Continued)[a]

glyco site	peptide and enzyme used	HPLC fraction	molecular mass of peptide (Da)			molecular mass after neuraminidase (Da)		proposed carbohydrate attached
			theoretical without carbohydrate	observed	theoretical with carbohydrate	observed	theoretical	
Asn^{86}	Asp^{78}−Asn^{86} AspN/Tryp	14	1058.16	3921.33 3629.34 3336.90	3920.76 3629.50 3338.24	3338.06 (incomplete digest)	3046.99	complex tri-antennary + 1−3 NeuAc
Asn^{86}	Asp^{78}−Asn^{86} AspN	10	1058.16	3956.7 3667.2 3375.3	3953.79 3662.53 3371.26	3374.65	3371.26	hybrid di-antennary bisecting GlcNAc 6 mannose + 0−2 NeuAc
Asn^{86}	Asp^{78}−Asn^{86} AspN	14	1058.16	4431.30 4141.02 3849.00	4432.24 4140.98 3849.72 3558.47	3844.99 (incomplete digest)	3558.47	complex tetra-antennary 1 fucose + 0−3 NeuAc
Asn^{219}	Asn^{219}−Arg^{220} AspN/Tryp	3	288.31	3427.00 3135.10 2842.42	3435.17 3143.91 2852.65	2855.30	2852.65	hybrid di-antennary 2 fucose 7 mannose + 0−2 NeuAc
Asn^{219}	Asn^{219}−Arg^{220} AspN/Tryp	9	288.31	3798.95 3505.20 3214.35	3793.52 3502.26 3211.01	3213.20	3211.01	complex penta-antennary bisecting GlcNac + 0−2 NeuAc
Asn^{219}	Asn^{219}−Arg^{220} AspN/Tryp	11	288.31	3221.59 2928.58 2638.21	3224.99 2933.73 2642.47	2928.10 (incomplete digest)	2642.47	complex tetra-antennary + 0−2 NeuAc
Asn^{219}	Asn^{219}−Arg^{220} AspN/Tryp	17	288.31	3637.26 3345.96 3053.96	3638.36 3347.11 3055.85	3053.56	3055.85	hybrid di-antennary bisecting GlcNAc 2 fucose 7 mannose + 0−2 NeuAc

[a] Reduced and alkylated TAFI was digested with AspN or AspN/Tr. The N-glycosylated peptides were isolated by concanavalin A affinity chromatography and further separated by RP-HPLC. Subsequently, the peptide masses were measured by MALDI−TOF mass spectrometry. Aliquots were removed and digested with neuraminidase, and the mass were determined as indicated. The carbohydrate structures were deduced from the mass changes using GPMAW (Lighthouse data). All five potential N-glycosylation sites are used. Microheterogeneity was detected in Asn51, Asn63, Asn86, and Asn219. Abbreviation used: ND, not determined; hybrid, hybrid-type glycosylation; mono-ant, mono-antennary; di-ant, di-antennary; tri-ant, tri-antennary; tetra-ant, tetra-antennary; penta-ant, penta-antennary; complex, complex-type glycosylation; GlcNAc, *N*-acetylglucosamine; NeuAc, *N*-acetyl neuraminic acid; Man, mannose; Fuc, fucose.

The main structures found were a tri-antennary complex type (83%) and a complex tetra-antennary type with Fuc (11%). In addition, a hybrid type with two antennas, a bisecting GlcNAc, and six Man (6%) was also observed. Treatment with neuraminidase verified the structures (Table 1).

Structures of Asn219-Linked Glycans. Asn219 is the only glycosylation site situated in TAFIa. The attached glycans were heterogeneous (Table 1 and Figure 6). The main type of glycans attached were hybrid di-antennary type with seven Man, two Fuc, and a bisecting GlcNAc attached (59%). Furthermore, the same structure was found in a form lacking the bisecting GlcNAc (5%). In addition, a complex tetra-antennary type (27%) and a complex penta-antennary type with a bisecting GlcNAc (9%) were also found. Neuraminidase treatment verified the structures (Table 1). In addition, an unglycosylated peptide containing Asn219 was purified. This suggests that TAFIa exist in both a glycosylated and unglycosylated form.

Purification of Disulfide and Cys-Containing Peptides. In contrast to pancreatic procarboxypeptidase B, TAFI is unstable following activation. Because the structural integrity of many proteins depends upon disulfide bridges, a variation in the pattern could explain the difference in enzymatic stability of TAFIa. To investigate the disulfide connectivity, TAFI was alkylated and digested with trypsin, chymotrypsin, or Spase V8 as described in the Experimental Procedures. The resulting peptides were separated by gel-filtration chromatography (Figure 5A) and further purified by RP-HPLC chromatography (not shown). The purified peptides were characterized by a combination of MALDI−MS and Edman degradation.

Cys69. The only Cys residue in the activation peptide is Cys69. Because the activation peptide is released upon activation, Cys69 is most likely not involved in a disulfide bridge. The tryptic peptide containing Cys69 (Ala60−Arg92) contained two attached glycans (Asn63 and Asn86) and eluted early from the gel-filtration column (Figure 5A). The peptide was further purified by RP-HPLC and analyzed by MALDI−MS following enzymatic deglycosylation and automated Edman degradation. The observed mass of the peptide was 3591.05 Da (Table 2). The theoretical mass of the alkylated peptide was 3588.81 Da. The 2-Da discrepancy is caused by the PNGase F deglycosylation (+1 Da for each glycosylation site). These results confirm that Cys69 is not involved in a disulfide bridge and that Cys69 contains a free sulfhydryl group in native pro-TAFI, available for alkylation by iodoacetamide.

Cys156 and Cys169. The peptides containing Cys156 and Cys169 were not detected in the trypsin digest. This was most likely caused by the hydrophobic nature of the tryptic peptide (Glu162−Arg191) containing Cys169. It is likely that this hydrophobic peptide was unable to elute from the

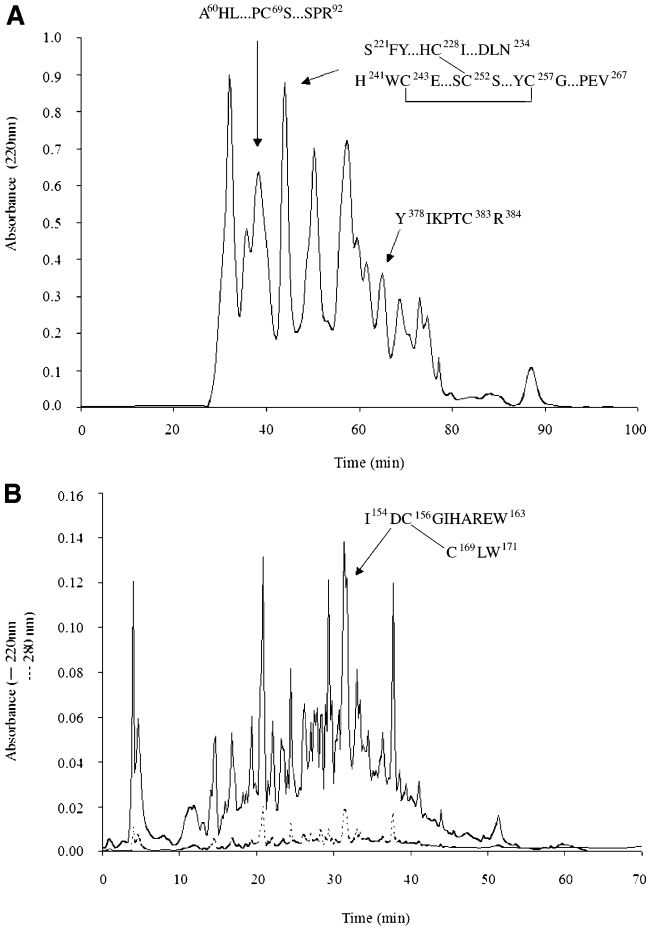

FIGURE 5: (A) Isolation of cysteine peptides. Alkylated TAFI was digested with trypsin, and the peptides were purified by a combination of gel filtration (Superdex Peptide HR 10/30) and RP-HPLC (not shown). The purified peptides were analyzed by MALDI−MS and Edman degradation to identify cysteine or cystine-containing peptides. The peaks containing the cysteines Cys69 and Cys383 and the cystines Cys228−Cys252 and Cys243−Cys257 are indicated. The peptides containing Cys156−Cys169 were not found because of the hydrophobic nature of the tryptic peptide containing Cys156. (B) Purification of the chymotryptic peptide containing Cys156. The chymotryptic digest was separated directly by RP-HPLC, and the peptides were identified by MALDI−MS and Edman degradation. Peptides were detected at both 220 and 280 nm as indicated. The peptides in question contained aromatic residues facilitating the detection at 280 nm.

RP-HPLC column. Instead, TAFI was digested by chymotrypsin, and the generated peptides were separated directly by RP-HPLC (Figure 5B). The chymotrypsin peptides of interest (Ile154−Trp163 and Cys169−Trp171) were significantly less hydrophobic and were identified by a combination of absorbance at 280 nm, MALDI−MS, and Edman degradation (Figure 5B). The mass of the unreduced sample (1617.71 Da) corresponded to the theoretical mass (1617.74 Da) of the two linked peptides (Table 2). The mass of the reduced sample (1256.58 Da) was consistent with the alkylation of Cys156 and release of the Cys169−Trp171 peptide. This confirms the disulfide bridge between Cys156 and Cys169.

Cys228, Cys252, Cys243, and Cys257. The tryptic peptides containing Cys228, Cys252, Cys243, and Cys257 eluted in the same fraction following gel-filtration chromatography (Figure 5A). Edman degradation and MALDI−MS analyses (4532.80 Da) confirmed that the fraction was composed of disulfide-linked peptides. To assign the disulfide bridges, the disulfide-linked peptides were subdigested using SPaseV8. The digest was separated by RP-HPLC, and the fractions were analyzed by MALDI−MS and Edman degradation. The peptide containing Cys228 and Cys252 coeluted from the RP-HPLC column. Similarly, the peptides containing Cys243 and Cys257 coeluted (data not shown). When the fractions were subjected to MALDI−MS analyses, the following masses were obtained, 1645.60 Da (His241−Glu245 and Thr255−Glu262), 2186.87 Da (His241−Glu245 and Thr255−Val267), and 2379.95 Da (Ser221−Asn234 and Gly246−Glu254). The aberrant C terminals of the Ser221−Asn234 and Thr255−Val267 peptides were most likely the result of trimming by residual TAFIa activity generated initially during tryptic digestion. This was further supported by analyses of the peptides in the reduced state (Table 2). In addition, the Cys243 and Cys257 disulfide-linked peptides existed in two cleavage variants producing masses of 1645.60 and 2186.87 Da. The masses and the Edman degradation data are consistent with disulfide bridges between Cys228 and Cys252 and between Cys243 and Cys257 (Table 2).

Cys383. The tryptic peptide (Tyr378−Arg384) containing Cys383 eluted late from the gel-filtration column (Figure 5A) and was identified by Edman degradation following RP-HPLC (Figure 5A). The peptide was analyzed by MALDI−MS, and the mass (937.48 Da) confirms that Cys383 contains a free sulfhydryl group in native TAFI available for alkylation by iodoacetamide.

Analysis of Post-translational Modifications Covering 90% of the TAFI Sequence Revealed only N-Linked Glycans and Disulfide Bridges. The LC−MS/MS analyses of TAFI covered 90% of the sequence and were consistent with the glycosylation of Asn22, Asn51, Asn63, Asn86, and Asn219. No other post-translational additions were detected (data not shown). The only exceptions were oxidations or deamidations, which are commonly observed nonenzymatic modifications often caused by handling during protein and peptide purifications. However, because some regions of TAFI were not covered by the analysis, we cannot exclude that TAFI contains other post-translational additions. Furthermore, modified peptides present in very low amounts relative to the nonmodified species could theoretically remain undetected by LC−MS/MS. However, the LC−MS/MS data revealed no evidence for post-translational modifications in TAFI other than the additions of glycans and formation of disulfide bridges.

DISCUSSION

The majority of the TAFI glycans are located on the activation peptide and account for approximately 20% of the overall size of the protein. The dissociation from the bulk of the molecule during activation causes the pI to shift from approximately 5 to 8 (Figure 1), rendering the protein significantly more basic and less soluble. All five potential N-linked glycosylation sites are occupied. Four of these sites, Asn51, Asn63, Asn86, and Asn219, display microheterogeneity in the carbohydrate structures attached (Figure 6). Some of the heterogeneity may also be caused by individual variations because TAFI was purified from pooled plasma. The carbohydrates varied between hybrid and complex types of glycosylation. Furthermore, varying amounts of Fuc and

Table 2: Identification of Cysteine Peptides[a]

			molecular mass of peptide (Da)			
			theoretical ($+^{+}$H)		observed ($+^{+}$H)	
cysteine	enzyme	peptide	−DTT	+DTT	−DTT	+DTT
Cys^{69}	Tr	$Ala^{60}-Arg^{92}$	3530.81	3531.81	3591.05	ND
Cys^{156}	Chymo	$Ile^{154}-Trp^{163}$	1617.74	1199.56	1617.71	1256.58
Cys^{169}		$Cys^{169}-Trp^{171}$		421.19	NA	NA
Cys^{228}	Tr	$Ser^{221}-Asn^{234}$	4532.82	1568.67	4532.80	1568.63
Cys^{243}		$His^{241}-Val^{267}$	(average)	2966.14	(average)	2966.17
Cys^{252}						
Cys^{257}						
Cys^{228}	Tr/V8	Ser^{221}-Asn^{234}	2379.95	1568.67	2379.95	ND
Cys^{252}		Gly^{246}-Glu^{254}		814.28		
Cys^{243}	Tr/V8	$His^{241}-Glu^{245}$	2186.87	703.24	2186.87	ND
Cys^{257}		$Thr^{255}-Val^{267}$		1486.24		
Cys^{243}	Tr/V8	$His^{241}-Glu^{245}$	1645.63	703.24	1645.60	ND
Cys^{257}		$Thr^{255}-Glu^{262}$		945.39		
Cys^{383}	Tr	$Tyr^{378}-Arg^{384}$	879.46	880.47	937.48	ND

[a] Peptides containing cysteine or cystine were purified by RP-HPLC and identified by Edman degradation, as described in the Experimental Procedures. MALDI−MS was employed to further analyze the peptides, either in their native form or following deglycosylation and/or reduction. Theoretical masses were obtained using GPMAW (Lighthouse data) and are derived from the amino acid sequence of the peptides. All masses are monoisotopic, unless otherwise indicated. Abbreviations used: NA, not applicable; ND, not determined.

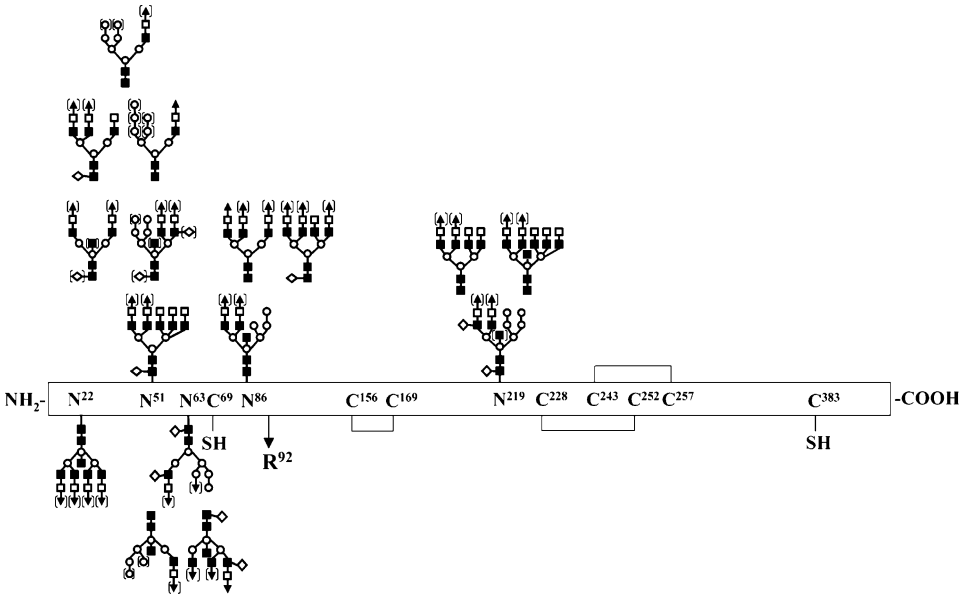

FIGURE 6: Schematic depicting the post-translational modifications of human plasma TAFI. The open bar represents mature TAFI including the identified post-translational modifications (not drawn to scale). The Arg92−Ala93 activation site is illustrated by an arrow. The disulfide bridges linking Cys156−Cys169, Cys228−Cys252, and Cys243−Cys257 are shown. Cys69 and Cys383 were found in the reduced state. All five potential N-linked glycosylation sites were utilized. The proposed carbohydrate structures are seen above each site. Most sites contain several different carbohydrate moieties, displaying microheterogeneity. The structures are based on calculations using GPMAW (Lighthouse data) and are only hypothetical in terms of the NeuAc position. The brackets indicate heterogeneity. Symbols: ■, GlcNAc; ○, Man; □, Gal; ▲, NeuAc and ◇, Fuc.

bisecting GlcNAc were found in each carbohydrate attachment site. The fifth site, Asn22, located in the activation peptide, contained only the tetra-antennary complex type with bisecting GlcNAc.

It has been suggested that TAFI carries O-linked glycans (*31*). However, monosaccharide composition analysis and LC−MS/MS failed to detect O-linked glycosylations. Asn219 was identified both in a glycosylated and unglycosylated form. Asn219 is positioned in close proximity to some of the proposed substrate-binding residues (Arg214, Arg217, and Lys218) in the primary sequence (*4*). The presence of a large hydrophilic glycan may alter the substrate-binding properties, and it can be speculated that the glycosylation of this site plays a role in the regulation of substrate binding.

It has previously been shown that TAFI is synthesized by the liver (*4*, *41*) and is released from platelets during platelet activation (*42*). Branched complex *N*-glycans are synthesized in the Golgi apparatus by *N*-acetylglucosaminyltransferases (GnT) I−VI. GnT III catalyzes the addition of a bisecting GlcNAc to the trimannose core. TAFI subtypes containing bisecting GlcNac's were identified in this study, and because GnT III is expressed only at very low levels in normal liver tissue (*43*−*45*), the origin of these TAFI subtypes in plasma are unclear. Platelet-derived TAFI migrates lower (50 kDa) than plasma TAFI (58 kDa) in SDS−PAGE, because of differences in glycosylation (*42*). The TAFI purified in this study migrated exclusively as a 58-kDa band, suggesting that it was not derived from the patelets. The bisecting GlcNAc

TAFI subtypes in plasma are thus not derived from platelets, suggesting that another source of plasma TAFI exists.

In contrast to the homologous pancreatic carboxypeptidase B, the enzymatic activity of TAFIa is short-lived. Inactivation takes place by both a cleavage in the C terminal and a spontaneous temperature-dependent structural change of the protein (*4*, *6*, *9*, *31*). Disulfides are a major contributor to the structural integrity of proteins, and disulfide permutations could explain the difference in enzymatic stability between TAFIa and pancreatic carboxypeptidase B. We determined three intrachain disulfide bonds located between Cys156−Cys169, Cys228−Cys252, and Cys243−Cys257 in human TAFI. In addition, Cys69 and Cys383 were found to contain free sulfhydryl groups. All cysteine residues, except Cys69, are conserved in human and porcine pancreatic procarboxypeptidase B. The disulfide connectivity described in this study is consistent with the predicted disulfide-bridge pattern previously described (*35*).

TAFI shares ~40% overall sequence identity with both human and porcine pancreatic procarboxypeptidase B. The conservation of the disulfide connectivity corroborates the notion that the catalytic domain of TAFI (TAFIa) is similar to pancreatic carboxypeptidase B. However, the activation peptides share only 20% of the amino acid residues. In addition, as determined in this study, the TAFI activation peptide is heavily glycosylated, carrying four large N-linked glycans. Thus far, no structural data of the protein is available, but a TAFI model has been proposed on the basis of the high degree of sequence identity between TAFI and other procarboxypeptidases (*35*). This model suggests that the activation peptide of TAFI has the same globular fold as pancreatic procarboxypeptidase A and B.

In this study, we have identified and characterized the post-translational modifications of authentic TAFI purified from human plasma. The disulfide connectivity was homologous to pancreatic carboxypeptidase B. Additional post-translational modifications included five N-linked glycans, four attached to the activation peptide and one to the catalytic domain close to residues involved in substrate binding. The activation of TAFI dissociates the activation peptide and removes the bulk of the attached glycans. This had a profound effect on the properties of TAFIa, including a shift in the pI from the acidic to basic range and a reduction in solubility.

ACKNOWLEDGMENT

We thank Drs. Henrik Karring and Steen V. Petersen for helpful discussions during the course of this work.

REFERENCES

1. Hendriks, D., Scharpe, S., van Sande, M., and Lommaert, M. P. (1989) A labile enzyme in fresh human serum interferes with the assay of carboxypeptidase N, *Clin. Chem. 35*, 177.
2. Hendriks, D., Scharpe, S., van Sande, M., and Lommaert, M. P. (1989) Characterisation of a carboxypeptidase in human serum distinct from carboxypeptidase N, *J. Clin. Chem. Clin. Biochem. 27*, 277−285.
3. Hendriks, D., Wang, W., Scharpe, S., Lommaert, M. P., and van Sande, M. (1990) Purification and characterization of a new arginine carboxypeptidase in human serum, *Biochim. Biophys. Acta 1034*, 86−92.
4. Eaton, D. L., Malloy, B. E., Tsai, S. P., Henzel, W., and Drayna, D. (1991) Isolation, molecular cloning, and partial characterization of a novel carboxypeptidase B from human plasma, *J. Biol. Chem. 266*, 21833−21838.
5. Redlitz, A., Tan, A. K., Eaton, D. L., and Plow, E. F. (1995) Plasma carboxypeptidases as regulators of the plasminogen system, *J. Clin. Invest. 96*, 2534−2538.
6. Bajzar, L., Morser, J., and Nesheim, M. (1996) TAFI, or plasma procarboxypeptidase B, couples the coagulation and fibrinolytic cascades through the thrombin−thrombomodulin complex, *J. Biol. Chem. 271*, 16603−16608.
7. Sakharov, D. V., Plow, E. F., and Rijken, D. C. (1997) On the mechanism of the antifibrinolytic activity of plasma carboxypeptidase B, *J. Biol. Chem. 272*, 14477−14482.
8. Mosnier, L. O., Meijers, J. C., and Bouma, B. N. (2001) Regulation of fibrinolysis in plasma by TAFI and protein C is dependent on the concentration of thrombomodulin, *Thromb. Haemostasis 85*, 5−11.
9. Wang, W., Hendriks, D. F., and Scharpe, S. S. (1994) Carboxypeptidase U, a plasma carboxypeptidase with high affinity for plasminogen, *J. Biol. Chem. 269*, 15937−15944.
10. Bouma, B. N., and Meijers, J. C. (2003) Thrombin-activatable fibrinolysis inhibitor (TAFI, plasma procarboxypeptidase B, procarboxypeptidase R, procarboxypeptidase U), *J. Thromb. Haemostasis 1*, 1566−1574.
11. Hendriks, D. F. (2004) *Carboxypeptidase U*, Elsevier, London, U.K.
12. Matsumoto, A., Itoh, K., and Matsumoto, R. (2000) A novel carboxypeptidase B that processes native β-amyloid precursor protein is present in human hippocampus, *Eur. J. Neurosci. 12*, 227−238.
13. Kremer Hovinga, J. A., Franco, R. F., Zago, M. A., Ten Cate, H., Westendorp, R. G., and Reitsma, P. H. (2004) A functional single nucleotide polymorphism in the thrombin-activatable fibrinolysis inhibitor (TAFI) gene associates with outcome of meningococcal disease, *J. Thromb. Haemostasis 2*, 54−57.
14. Reynolds, D. S., Gurley, D. S., Stevens, R. L., Sugarbaker, D. J., Austen, K. F., and Serafin, W. E. (1989) Cloning of cDNAs that encode human mast cell carboxypeptidase A, and comparison of the protein with mouse mast cell carboxypeptidase A and rat pancreatic carboxypeptidases, *Proc. Natl. Acad. Sci. U.S.A. 86*, 9480−9484.
15. Catasus, L., Vendrell, J., Aviles, F. X., Carreira, S., Puigserver, A., and Billeter, M. (1995) The sequence and conformation of human pancreatic procarboxypeptidase A2. cDNA cloning, sequence analysis, and three-dimensional model, *J. Biol. Chem. 270*, 6651−6657.
16. Catasus, L., Villegas, V., Pascual, R., Aviles, F. X., Wicker-Planquart, C., and Puigserver, A. (1992) cDNA cloning and sequence analysis of human pancreatic procarboxypeptidase A1, *Biochem. J. 287* (part 1), 299−303.
17. Yamamoto, K. K., Pousette, A., Chow, P., Wilson, H., el Shami, S., and French, C. K. (1992) Isolation of a cDNA encoding a human serum marker for acute pancreatitis. Identification of pancreas-specific protein as pancreatic procarboxypeptidase B, *J. Biol. Chem. 267*, 2575−2581.
18. Auld, D. (2004) *Catalytic Mechanisms of Metallopeptidases*, Elsevier, London, U.K.
19. Valnickova, Z., Thogersen, I. B., Christensen, S., Chu, C. T., Pizzo, S. V., and Enghild, J. J. (1996) Activated human plasma carboxypeptidase B is retained in the blood by binding to α2-macroglobulin and pregnancy zone protein, *J. Biol. Chem. 271*, 12937−12943.
20. Valnickova, Z., and Enghild, J. J. (1998) Human procarboxypeptidase U, or thrombin-activable fibrinolysis inhibitor, is a substrate for transglutaminases. Evidence for transglutaminase-catalyzed cross-linking to fibrin, *J. Biol. Chem. 273*, 27220−27224.
21. Wang, W., Boffa, M. B., Bajzar, L., Walker, J. B., and Nesheim, M. E. (1998) A study of the mechanism of inhibition of fibrinolysis by activated thrombin-activable fibrinolysis inhibitor, *J. Biol. Chem. 273*, 27176−27181.
22. Fleury, V., and Angles-Cano, E. (1991) Characterization of the binding of plasminogen to fibrin surfaces: The role of carboxy-terminal lysines, *Biochemistry 30*, 7630−7638.
23. Cesarman, G. M., Guevara, C. A., and Hajjar, K. A. (1994) An endothelial cell receptor for plasminogen/tissue plasminogen activator (t-PA). II. Annexin II-mediated enhancement of t-PA-dependent plasminogen activation, *J. Biol. Chem. 269*, 21198−21203.
24. Pannell, R., Black, J., and Gurewich, V. (1988) Complementary modes of action of tissue-type plasminogen activator and pro-

urokinase by which their synergistic effect on clot lysis may be explained, *J. Clin. Invest. 81*, 853−859.
25. Christensen, U. (1985) C-terminal lysine residues of fibrinogen fragments essential for binding to plasminogen, *FEBS Lett. 182*, 43−46.
26. Hoylaerts, M., Rijken, D. C., Lijnen, H. R., and Collen, D. (1982) Kinetics of the activation of plasminogen by human tissue plasminogen activator. Role of fibrin, *J. Biol. Chem. 257*, 2912−2919.
27. Tan, A. K., and Eaton, D. L. (1995) Activation and characterization of procarboxypeptidase B from human plasma, *Biochemistry 34*, 5811−5816.
28. Mao, S. S., Cooper, C. M., Wood, T., Shafer, J. A., and Gardell, S. J. (1999) Characterization of plasmin-mediated activation of plasma procarboxypeptidase B. Modulation by glycosaminoglycans, *J. Biol. Chem. 274*, 35046−35052.
29. Boffa, M. B., Bell, R., Stevens, W. K., and Nesheim, M. E. (2000) Roles of thermal instability and proteolytic cleavage in regulation of activated thrombin-activable fibrinolysis inhibitor, *J. Biol. Chem. 275*, 12868−12878.
30. Marx, P. F., Hackeng, T. M., Dawson, P. E., Griffin, J. H., Meijers, J. C., and Bouma, B. N. (2000) Inactivation of active thrombin-activable fibrinolysis inhibitor takes place by a process that involves conformational instability rather than proteolytic cleavage, *J. Biol. Chem. 275*, 12410−12415.
31. Boffa, M. B., Wang, W., Bajzar, L., and Nesheim, M. E. (1998) Plasma and recombinant thrombin-activable fibrinolysis inhibitor (TAFI) and activated TAFI compared with respect to glycosylation, thrombin/thrombomodulin-dependent activation, thermal stability, and enzymatic properties, *J. Biol. Chem. 273*, 2127−2135.
32. Zhao, L., Morser, J., Bajzar, L., Nesheim, M., and Nagashima, M. (1998) Identification and characterization of two thrombin-activatable fibrinolysis inhibitor isoforms, *Thromb. Haemostasis 80*, 949−955.
33. Brouwers, G. J., Vos, H. L., Leebeek, F. W., Bulk, S., Schneider, M., Boffa, M., Koschinsky, M., van Tilburg, N. H., Nesheim, M. E., Bertina, R. M., and Gomez Garcia, E. B. (2001) A novel, possibly functional, single nucleotide polymorphism in the coding region of the thrombin-activatable fibrinolysis inhibitor (TAFI) gene is also associated with TAFI levels, *Blood 98*, 1992−1993.
34. Schneider, M., Boffa, M., Stewart, R., Rahman, M., Koschinsky, M., and Nesheim, M. (2002) Two naturally occurring variants of TAFI (Thr-325 and Ile-325) differ substantially with respect to thermal stability and antifibrinolytic activity of the enzyme, *J. Biol. Chem. 277*, 1021−1030.
35. Barbosa Pereira, P. J., Segura-Martin, S., Oliva, B., Ferrer-Orta, C., Aviles, F. X., Coll, M., Gomis-Ruth, F. X., and Vendrell, J. (2002) Human procarboxypeptidase B: Three-dimensional structure and implications for thrombin-activatable fibrinolysis inhibitor (TAFI), *J. Mol. Biol. 321*, 537−547.
36. Wiman, B. (1980) Affinity-chromatographic purification of human α 2-antiplasmin, *Biochem. J. 191*, 229−232.
37. Bury, A. F. (1981) Analysis of protein and peptide mixtures. Evaluation of three sodium dodecyl sulphate−polyacrylamide gel electrophoresis buffer systems, *J. Chromatogr. 213*, 491−500.
38. Matsudaira, P. (1987) Sequence from picomole quantities of proteins electroblotted onto polyvinylidene difluoride membranes, *J. Biol. Chem. 262*, 10035−10038.
39. Hendriks, D., Scharpe, S., and van Sande, M. (1985) Assay of carboxypeptidase N activity in serum by liquid-chromatographic determination of hippuric acid, *Clin. Chem. 31*, 1936−1939.
40. Perkins, D. N., Pappin, D. J., Creasy, D. M., and Cottrell, J. S. (1999) Probability-based protein identification by searching sequence databases using mass spectrometry data, *Electrophoresis 20*, 3551−3567.
41. Vanhoof, G., Wauters, J., Schatteman, K., Hendriks, D., Goossens, F., Bossuyt, P., and Scharpe, S. (1996) The gene for human carboxypeptidase U (CPU)—A proposed novel regulator of plasminogen activation—Maps to 13q14.11, *Genomics 38*, 454−455.
42. Mosnier, L. O., Buijtenhuijs, P., Marx, P. F., Meijers, J. C., and Bouma, B. N. (2003) Identification of thrombin activatable fibrinolysis inhibitor (TAFI) in human platelets, *Blood 101*, 4844−4846.
43. Nishikawa, A., Fujii, S., Sugiyama, T., and Taniguchi, N. (1988) A method for the determination of *N*-acetylglucosaminyltransferase III activity in rat tissues involving HPLC, *Anal. Biochem. 170*, 349−354.
44. Nishikawa, A., Fujii, S., Sugiyama, T., Hayashi, N., and Taniguchi, N. (1988) High expression of an *N*-acetylglucosaminyltransferase III in 3′-methyl DAB-induced hepatoma and ascites hepatoma, *Biochem. Biophys. Res. Commun. 152*, 107−112.
45. Nishikawa, A., Gu, J., Fujii, S., and Taniguchi, N. (1990) Determination of *N*-acetylglucosaminyltransferases III, IV, and V in normal and hepatoma tissues of rats, *Biochim. Biophys. Acta 1035*, 313−318.

BI051956V